NANO LETTERS

pubs.acs.org/NanoLett

Detection of Nucleic Acids with Graphene Nanopores: Ab Initio Characterization of a Novel Sequencing Device

Tammie Nelson, Bo Zhang, and Oleg V. Prezhdo*

Department of Chemistry, University of Washington, Seattle, Washington 98195-1700

ABSTRACT We report an ab initio density functional theory study of the interaction of four nucleobases, cytosine, thymine, adenine, and guanine, with a novel graphene nanopore device for detecting the base sequence of a single-stranded nucleic acid (ssDNA or RNA). The nucleobases were inserted into a pore in a graphene nanoribbon, and the electrical current and conductance spectra were calculated as functions of voltage applied across the nanoribbon. The conductance spectra and charge densities were analyzed in the presence of each nucleobase in the graphene nanopore. The results indicate that due to significant differences in the conductance spectra the proposed device has adequate sensitivity to discriminate between different nucleotides. Moreover, we show that the nucleotide conductance spectrum is affected little by its orientation inside the graphene nanopore. The proposed technique may be extremely useful for real applications in developing ultrafast, low-cost DNA sequencing methods.

KEYWORDS Nucleic acid, sequencing, graphene, electrical current, conductance spectroscopy, density functional theory

Recent advances in the biomedical industry and research have stimulated an increasing demand to develop fast and inexpensive methods for DNA analysis. Devices with nanometer-sized pores have become the subject of intense study as they continue to open up new avenues for DNA sequencing. Nanopore-based sequencing methods were first proposed by Kasianowicz et al.[1] more than a decade ago with the use of α-hemolysin protein pores inserted into a lipid membrane. Since then, numerous studies have been reported using protein nanopores. Focus has recently shifted to solid-state nanopores. They have emerged as promising sensors that are mechanically robust, integrate well with electronics, can be fabricated rapidly, and allow nanopore diameter and surface properties to be fine-tuned.[2−5] The ionic-current blockade method has been extended to materials such as SiO_2, Al_2O_3, and Si_3N_4.[6−9]

In a typical experiment, individual ssDNA or RNA molecules are electrophoretically driven through a pore and the resulting ionic-current blockade is measured.[2,10−15] Because of differences in the size of nucleotides and their interaction with the pore, the ionic-current is anticipated to vary when each nucleotide is driven through. However, a number of challenges have been recognized, which need to be addressed before nanopores can be utilized to sequence DNA. These challenges include finite thickness of the translocation zone, fast speed of DNA translocation, and low bandwidth in recording of the ionic-current.[16] Several new methods based on nanopores have recently been proposed to sequence ssDNAs at high speed.[17−19] One of the most interesting methods is based on the measurement of the tunneling-current through a pair of nanoelectrodes placed at the nanopore opening.[20−24] In this type of experiment the tunneling-current could be extremely sensitive to the orientation of the nucleotides in the nanopore.

In this letter we explore a device based on the idea of measuring the electrical current perpendicular to the DNA backbone resulting from the translocation of ssDNA in solution through a solid-state nanopore. We propose a novel device containing a graphene nanopore (GNP) created from a single-layered graphene nanoribbon (GNR) embedded in SiO_2, as depicted in Figure 1. We envision that each of the DNA bases will produce a unique current that can be

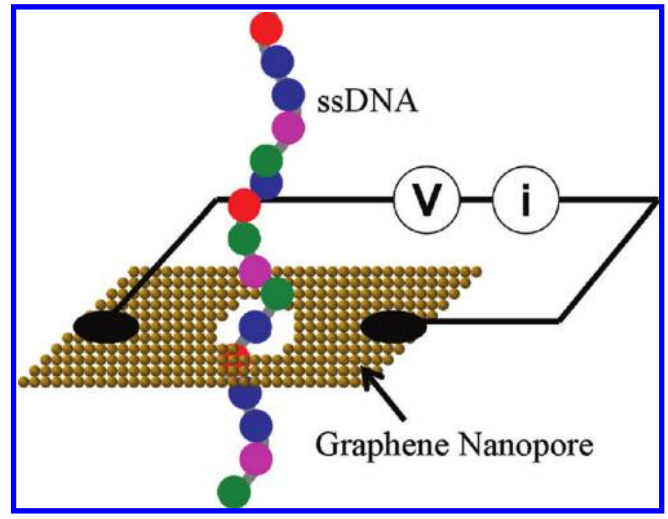

FIGURE 1. Proposed nanopore sensor consists of a graphene nanopore embedded in SiO_2 (not pictured). Single-stranded DNA translocate through the nanopore. The current flow is perpendicular to the DNA backbone.

* To whom correspondence should be addressed. E-mail: prezhdo@uw.edu.
Received for review: 10/27/2009
Published on Web: 08/19/2010

DOI: 10.1021/nl9035934 | *Nano Lett.* **2010,** *10,* 3237–3242

measured as it passes through the pore. Creating such a device is now possible by the established methods of graphene fabrication.[25−28] Ab initio density-functional theory (DFT) was used to calculate electrical current and conductance through the proposed device and to predict its feasibility. The following two requirements for device performance must be met: (1) there must be a sufficient difference in the conductance spectra $G(V)$ of individual nucleobases to allow them to be distinguished from one another, and (2) the measured conductance for a single nucleobase must be independent of its orientation as it passes through the pore. Otherwise, the noise introduced by the orientation dependence of the signal can present a serious problem. The second requirement has been largely overlooked in previous studies. The results will show that our GNP device meets both of these requirements.

Electronic structure calculations were used to determine the transverse electrical current for nine model systems with optimized geometry (Figure 2); starting with a semiconducting ideal GNR[29−33] (iGNR), we first created a pore in the center of the ribbon (GNP) and then inserted cytosine into the pore (cGNP). The effect of molecule orientation was then investigated by rotating the cytosine by 90° along the axis perpendicular to the ribbon, rotated cGNP (rcGNP), by 90° into the ribbon plane, planar cGNP (pcGNP), and by 90° into the ribbon plane, tilted cGNP (tcGNP). The ability of the proposed device to detect the molecular identity was investigated by replacing cytosine with adenine (aGNP), guanine (gGNP), and thymine (tGNP). The detection of sugar and phosphate groups forming a DNA chain was studied as well; see Supporting Information. The Supporting Information also investigates the effect of the nearest-neighbor interactions in the DNA chain on the conductance spectra. The calculations were preformed with the Vienna Ab Initio Simulations Package[34,35] using the generalized gradient approximation of Perdew, Burke, and Ernzerhof[36] and the projector augmented-wave method.[37] All of the ribbons were constructed with hydrogen-terminated armchair edges and have a width of 3.3 nm in the y-direction while being continuous in the x-direction. Current flow occurs in the x-direction while DNA translocation is along the z-direction. Periodic boundary conditions were implemented with sufficient vacuum in the y and z-directions to avoid spurious ribbon−ribbon interactions. The nanopore measures 1.45 nm in diameter and is composed of both armchair and zigzag edges terminated with hydrogen.[38] The nucleobases were constructed with a methyl group at the cut bond to the backbone in place of the more traditional hydrogen. This was done to create an electronic and steric environment more similar to DNA. Ions and solvating water molecules were not included in our idealized simulations. Minimum energy structures were obtained for the iGNR and GNP by relaxing the ribbon geometry and simulation cell. We chose not to further optimize the GNP around the nucleobases because our test revealed an insignificant difference in the band structure between initial optimization and subsequent optimization of the pore. The density of states (DOS) was then calculated with DFT and was used to compute current and conductance.

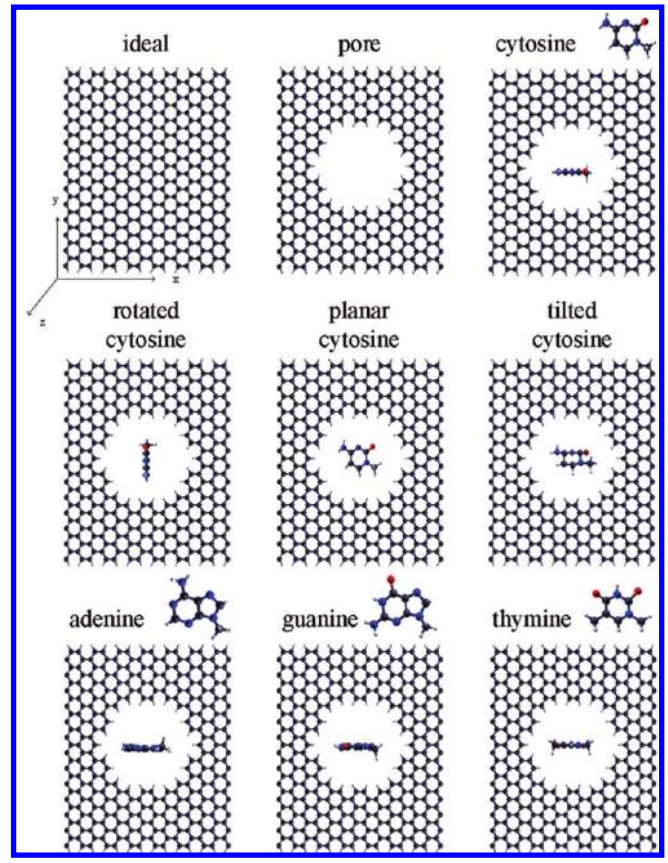

FIGURE 2. Model systems used for our analysis. Gray, white, blue, and red spheres represent carbon, hydrogen, nitrogen, and oxygen, respectively. First row: Starting with an ideal GNR (left) we first created a 1.45 nm pore in the ribbon (center). Then cytosine was placed in the pore (right). Second row: Orientation of the nucelobase was investigated using cytosine. The cytosine molecule was rotated about the z-axis by 90° (left). Cytosine was then placed in a planar configuration by rotating 90° about the x-axis (center) followed by an intermediate tilted configuration achieved by a 45° rotation about the x-axis (right). Bottom row: The three remaining nucleobases adenine (left), guanine (center), and thymine (right) were then placed in the pore.

Molecular conductance has been extensively studied, and its theory is well-known.[39,40]

We begin our analysis by calculating the transverse electrical current using the Landauer-Buttiker formula

$$I(E, V) = \frac{e}{\pi\hbar}\int_{-\infty}^{\infty} dE f(E)T(E) \qquad (1)$$

where $T(E)$ is the transmission probability and $f(E)$ is the Fermi distribution function. To simplify the calculation we assign the transmission probability the maximum value of unity and replace the Fermi distribution function with DOS, $\rho(E)$. The former assumption is justified, since the conducting

DOI: 10.1021/nl9035934 | *Nano Lett.* **2010,** *10,* 3237–3242

states are delocalized over the whole system, and since the molecules strongly interact with the GNP. The latter approximation implies that DOS is weakly dependent on the state occupations that are changing with applied voltage. The approximations do not affect the key conclusions of our proof-of-principle calculations. The current is calculated numerically from the integrated DOS

$$I(E, V) = \frac{e}{\pi\hbar}\int_0^E dE'\rho(E - E') \quad (2)$$

The conductance is the derivative of the current

$$G(V) = \frac{\partial I(V)}{\partial V} \quad (3)$$

It is inversely related to the resistance through Ohm's law.

We first considered the change in conductance induced by forming a nanopore and then inserting a nucleobase into the pore. Figure 3 compares the conductance for the iGNR, GNP, and cGNP. The current is also shown, since it is the property that is directly measured in experimental studies. The conductance scale is given on the left *y*-axis, while the current scale is given on the right *y*-axis. Note that the top and bottom panels have different *y*-axis scales. The conductance is greater in the iGNR than in the GNP. The charge density for the conduction channel at −1.15 V is shown in order to illustrate the origin of the difference in the conductance of the iGNR and GNP. The iGNR has a uniform distribution of density covering the entire ribbon. Creating the pore breaks the ribbon symmetry and generates an asymmetric density distribution. Some of the carbon atoms are removed, and the overall electron density decreases. In comparison, the asymmetry between conductance at the positive and negative biases[41] is reduced by the pore creation. It has previously been reported that the decrease in conductance will be directly related to the size of the pore.[8] Thus, it would be possible to determine the nanopore diameter by monitoring the conductance drop.

Insertion of cytosine into the pore induces partial recovery of the previous conductance loss; the conductance of cGNP is greater than GNP. Since the pore is notably larger in size than the molecule, and since the carbon dangling bonds are saturated, as expected in an aqueous environment or air, the molecule−ribbon interaction is electrostatic in nature. The molecule enhances GNP conductance by both providing additional conductance channels and attracting the charge density into the previously depleted GNP areas. The two effects are clearly illustrated with the electron density of cGNP responsible for the conduction channel at −1.70 V. The density is delocalized over both the molecule and GNP and covers the entire ribbon, similar to iGNR.

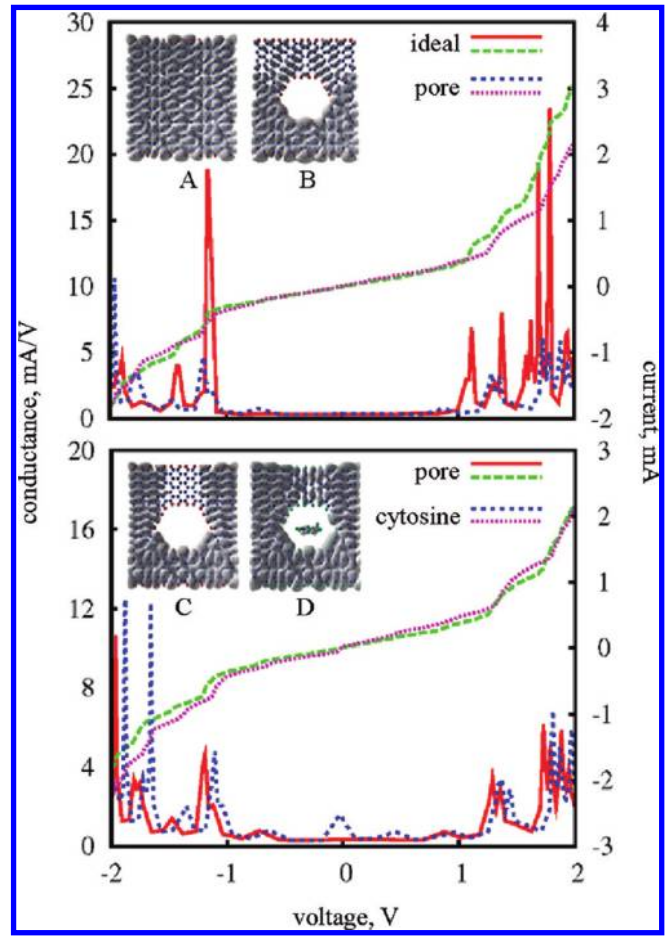

FIGURE 3. The effect of creating the nanopore and inserting a molecule is shown. The conductance (left axis) and current (right axis) are plotted for iGNR and GNP (top). The charge densities corresponding to the conduction channel at −1.15 V are shown for (A) iGNR and (B) GNP. Initial formation of the nanopore causes the current and conductance to drop, and the charge density transforms from an even to an asymmetric distribution. (bottom) GNP and cGNP. The charge densities corresponding to the conduction channel at −1.70 V are shown for (C) GNP and (D) cGNP. Insertion of the nucleobase cytosine into the pore causes the current and conductance to rise through an electrostatic molecule−ribbon interaction. Charge density is located on both the molecule and the surrounding ribbon.

Insertion of the molecule also causes the Fermi energy to increase. This effect is manifested as the slight shift in the conductance spectra. The Fermi energy shift offers another possible method of detection, as the change in the Fermi energy will be unique for each nucleobase.

Our next consideration was strand orientation. The calculations show that unlike tunneling-current devices,[20−23] the proposed GNP device is essentially insensitive to strand orientation. The top panel of Figure 4 compares the conductance for the cGNP and rcGNP, while the bottom panel shows the conductance for the pcGNP and tcGNP, see Figure 2 for a better view of the geometries of these four cytosine orientations. To determine whether the conductance is subject to the orientation of the DNA strand as it enters the nanopore, we rotated the cytosine by 90° perpendicular to

DOI: 10.1021/nl9035934 | *Nano Lett.* **2010,** *10,* 3237–3242

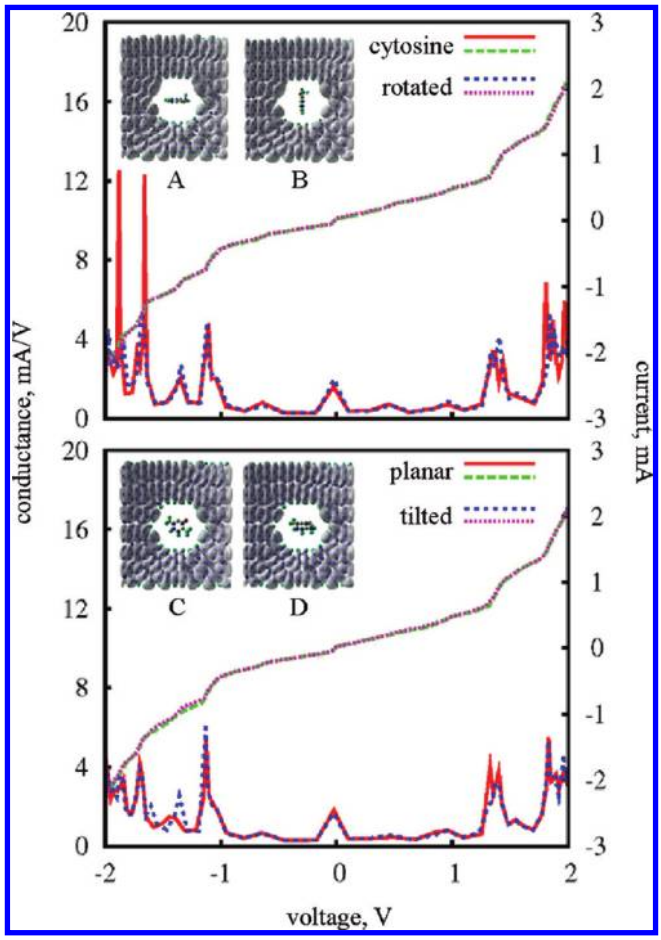

FIGURE 4. The effect of nucleobase orientation is shown. The conductance (left axis) and current (right axis) are plotted for cGNP and rotated cGNP (top), and for planar cGNP and tilted cGNP (bottom). The charge densities corresponding to the conduction channel at −1.10 V are shown for (A) cGNP, (B) rotated cGNP, (C) planar cGNP, and (D) tilted cGNP. Rotation of the cytosine molecule by 90 and 45° results in a relatively small change in the conductance and current of the ribbon with the largest deviation occurring for the planar configuration. Charge density remains evenly distributed on the ribbon before and after each rotation.

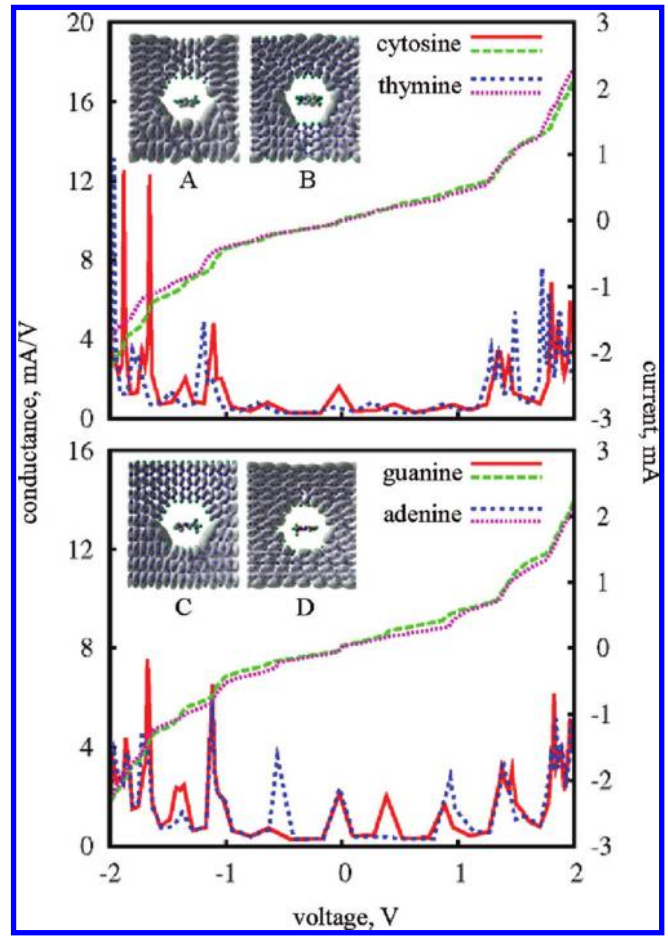

FIGURE 5. The four nucleobases are compared. The conductance (left axis) and current (right axis) are plotted for the pyrimidines cGNP and tGNP (top) and the purines gGNP and aGNP (bottom). The charge densities corresponding to the unique conduction channels are shown for (A) cGNP at −1.70 V, (B) tGNP at 1.48 V, (C) gGNP at 0.30 V, and (D) aGNP at −0.55 V. In each case, the charge density is located on both the molecule and the surrounding ribbon. The contribution from the molecule gives rise to a unique conduction channel that allows the nucleobases to be distinguished from one another.

the ribbon plane and into the ribbon plane. We also tilted the cytosine into the plane by 45°. The rotations leave the current and conductance spectra virtually unchanged and the charge density is also unaffected. The minor changes in the conductance spectra seen upon cytosine rotation are much less significant than the changes observed with nanopore creation and insertion of different nucleotides.

Our final consideration was the sensitivity of the proposed device to nucleotide type. Figure 5 presents the conductance spectra of all four nucleotides, while the Supporting Information shows the spectra of sugar and phosphate. The currents and conductances of the nanopores containing each of the four nucleotides and phosphate group are clearly distinct from each other and from those of the bare nanopore. Compared to the bare nanopore, there are no new peaks associated with the sugar within the considered voltage range. Generally, the purines gGNP and aGNP exhibit more conduction channels than the pyrimidines cGNP and tGNP, since the former are bigger molecules than the latter, and therefore, they contain a larger number of molecular orbitals within the relevant energy range. We also considered the effect of adjacent nucleotides and phosphate groups on the conduction of the nanopore containing cytosine; see Supporting Information. The calculations showed that neutral nucleotides and phosphate placed several angstroms away from the nanopore, as expected in a DNA chain passing through the pore, have little effect on the conductance spectra. The spectra do shift in the presence of charged phosphates; however, the overall spectral shapes change little, indicating that individual nucleotides can be efficiently detected by the proposed device regardless of nearby charges.

The GNP device has the potential to offer great improvements in sensitivity over ionic-current and tunneling-current devices. Current and conductance measurements in the

DOI: 10.1021/nl9035934 | Nano Lett. 2010, 10, 3237–3242

proposed GNP device are on the order of mA, since the device presents a single continuous nanowire. Its counterparts report current measurements on the order of μA, nA, and pA.[2,6−24] It is likely that the mA currents calculated for the present device are an overestimation, due to the idealistic setup which excludes various sources of dissipation, such as charge scattering[42] and electron−phonon interactions[35,40,43−45] Further, DFT can underestimate the nanopore band gap, and hence, overestimate the calculated current. Nevertheless, the band structure and relative current associated with nucleobases should change little.[46] Since GNR energy gaps decrease with increasing ribbon width,[29,30] wider GNRs have higher DOS and decrease device sensitivity to molecular energy levels.

Strong currents in the proposed device are favored by the fact that there remain continuous conduction channels through the ribbon itself, which is not completely broken in contrast to the conducting wires in the other devices.[20−24] In addition, the sizes of the molecule and the pore are of the same order, such that the molecule strongly interacts with the pore. The currents measured for the proposed device should be significantly higher than the ionic currents.[2,6−15] This is because the electrons in the graphene device move significantly faster than ions, both due to a smaller mass-to-charge ratio and a large charge scattering length. Clean nanotubes can exhibit ballistic conduction up to the micrometer scale,[45] while ionic scattering lengths are on the order of the intermolecular distance in liquids, that is, few angstroms. The presence of the pore and molecule will reduce the electron scattering length of the graphene ribbon to a few nanometers. Still, it will be substantially longer for electrons in the proposed device than for ions in a liquid.

A more realistic picture of the nanopore would have a mixture of armchair and zigzag edges with partial termination by hydrogens, oxygens, hydroxyls, and other species. With the limits of modern technology, it is impossible to ensure a symmetric and fully terminated nanopore edge, making actual current measurements different than predicted. The actual system will involve a substrate, a solvent, and DNA counterions.[47] Nucleotides, phosphates, and sugars will be adjacent to the main nucleotide and may affect the conductance spectra. The calculation results presented in the Supporting Information address some of these issues. The above factors will introduce noise into the current measurements. The magnitude of the signal-to-noise ratio can be estimated by considering the effect of the nucleotide rotation on the signal strength. Figures 4 and 5 show that the differences in the conduction due to nucleotide rotation, representing noise, are significantly smaller than the absolute values of the conductance. For the majority of the conduction peaks the signal-to-noise ratio estimated this way is greater than one by several orders of magnitude.

Most proposals for conductance-based nucleotide detection rely on tunneling currents that are mediated by the energy levels introduced by the nucleotide within a gap in a nanowire.[20−24] Our proposed device includes this detection mechanism, which shows particularly fine spatial resolution and little dependence on nucleotide rotation. Further, our device allows for an alternative detection mechanism. Conductance through the nanoribbon itself is modulated by electrostatic interaction of the nucleotide with the ribbon. This sensitivity is unique to our device due to its small size and the single-layer thickness. The two complementary detection mechanisms provide an additional advantage to the proposed device.

In summary, the proposed graphene nanopore device allows measurement of electrical current in the direction perpendicular to a translocating DNA and other molecules. The simulations have shown that the device meets both of the necessary performance requirements, confirming device feasibility; it is insensitive to strand orientation, and at the same time, it provides discrimination that is sufficient for nucleobase identification. Detection can be achieved by focusing on either particular regions of the conductance spectra or the changing Fermi energy. The study suggests that a graphene nanopore offers a robust and experimentally realizable technology for use in DNA sequence analysis. It provides strong motivation for the development of a new class of nanopore sequencing devices.

Acknowledgment. The authors are grateful to Dr. Bradley F. Habenicht for fruitful discussions. The research was supported by grants from NSF CHE-0701517 and ACS PRF 41436-AC6.

Supporting Information Available. Additional figures are presented. This material is available free of charge via the Internet at http://pubs.acs.org.

REFERENCES AND NOTES

(1) Kasianowicz, J. T.; Brandin, E.; Branton, D.; Deamer, D. W. *Proc. Natl. Acad. Sci. U.S.A.* **1996**, *93*, 13770.
(2) Deamer, D. W.; Branton, D. *Acc. Chem. Res.* **2002**, *35*, 817.
(3) Storm, A. J.; chen, J. H.; Ling, X. S.; Zandbergen, H. W.; Dekker, C. *Nat. Mater.* **2003**, *2*, 537.
(4) Chen, P.; Mitsui, T.; Farmer, D. B.; Golovchenko, J.; Gordon, R. G.; Branton, D. *Nano Lett.* **2004**, *4*, 1333.
(5) Kim, M. J.; Wanunu, M.; Bell, D. C.; Meller, A. *Adv. Mater.* **2006**, *18*, 3149.
(6) Chang, H.; Kosari, F.; Andreadakis, G.; Alam, M. A.; Vasmatzis, G.; Bashir, R. *Nano Lett.* **2004**, *4*, 1551.
(7) Fologea, D.; Gershow, M.; Ledden, B.; McNabb, D. S.; Golovchenko, J. A.; Li, J. *Nano Lett.* **2005**, *5*, 1905.
(8) Venkatesan, B. M.; Dorvel, B.; Yemenicioglu, S.; Watkins, N.; Petrov, I.; Bashir, R. *Adv. Mater.* **2009**, *21*, 2771.
(9) Heng, J. B.; Aksimentiev, A.; Ho, C.; Marks, P.; Grinkova, Y. V.; Sligar, S.; Schulten, K.; Timp, G. *Nano Lett.* **2005**, *5*, 1883.
(10) Deamer, D. W.; Akeson, M. *Trends Biotechnol.* **2000**, *18*, 147.
(11) Meller, A.; Nivon, L.; Branton, D. *Phys. Rev. Lett.* **2001**, *86*, 3435.
(12) Butler, T. Z.; Gundlach, J. H.; Troll, M. *Biophys. J.* **2007**, *93*, 3229.
(13) Hu, T.; Shklovskii, B. I. *Phys. Rev. E* **2008**, *78*, No. 032901.
(14) Butler, T. Z.; Pavlenok, M.; Derrington, I. M.; Niederweis, M.; Gundlach, J. H. *Proc. Natl. Acad. Sci. U.S.A.* **2008**, *105*, 20647.
(15) Stoddart, D.; Heron, A. J.; Mikhailova, E.; Maglia, G.; Bayley, H. *Proc. Natl. Acad. Sci. U.S.A.* **2009**, *106*, 7702.
(16) Branton, D.; Deamer, D. W.; Marziali, A.; Bayley, H.; Benner, S. A.; Butler, T.; Ventra, M. D.; Garaj, S.; Hibbs, A.; Huang, X.; Jovanovich, S. B.; Krstic, P. S.; Lindsay, S.; Ling, X. S.; Mastrangelo, C. H.;

DOI: 10.1021/nl9035934 | *Nano Lett.* **2010,** *10,* 3237–3242

Meller, A.; Oliver, J. S.; Pershin, Y. V.; Ramsey, J. M.; Soni, R. R. G. V.; Tabard-Cossa, V.; Wanunu, M.; Wiggin, M.; Schloss, J. A. *Nat. Biotechnol.* **2008**, *26*, 1146.
(17) Zwolak, M.; Ventra, M. D. *Nano Lett.* **2005**, *5*, 421.
(18) Sigalov, G.; Comer, J.; Timp, G.; Aksimentiev, A. *Nano Lett.* **2008**, *8*, 56.
(19) Lu, J. Q.; Zhang, X. G. *Biophys. J.* **2008**, *95*, L60.
(20) Lagerqvist, J.; Zwolak, M.; Ventra, M. D. *Nano Lett.* **2006**, *6*, 779.
(21) Zikic, R.; Krstic, P. S.; Zhang, X. G.; Fuentes-Cabrera, M.; Wells, J.; Zhao, X. *Phys. Rev. E* **2006**, *74*, No. 011919.
(22) Zhang, X. G.; Krstic, P. S.; Zikic, R.; Wells, J. C.; Fuentes-Cabrera, M. *Biophys. J.* **2006**, *91*, L04.
(23) Meunier, V.; Krstic, P. S. *J. Chem. Phys.* **2008**, *128*, No. 041103.
(24) Postma, H. W. C. *Nano Lett.* **2010**, *10*, 420.
(25) Novoselov, K. S.; Geim, A. K.; Morozov, S. V.; Jiang, D.; Zhang, Y.; Dubonos, S. V.; Grigorieva, I. V.; Firsov, A. A. *Science* **2004**, *306*, 666.
(26) Han, M. Y.; Barbaros, O.; Zhang, Y.; Kim, P. *Phys. Rev. Lett.* **2007**, *98*, 206805.
(27) Meyer, J. C.; Girit, C. O.; Crommie, M. F.; Zettl, A. *Appl. Phys. Lett.* **2008**, *92*, 123110.
(28) Girit, C. O.; Meyer, J. C.; Erni, R.; Rossell, M. D.; Kisielowski, C.; Yang, L.; Park, C. H.; Crommie, M. F.; Cohen, M. L.; Louie, S. G.; Zettl, A. *Science* **2009**, *323*, 1705.
(29) Son, Y. W.; Cohen, M. L.; Louie, S. G. *Phys. Rev. Lett.* **2006**, *97*, 216803.
(30) Barone, V.; Hod, O.; Scuseria, G. E. *Nano Lett.* **2006**, *6*, 2748.
(31) Hod, O.; Scuseria, G. E. *Nano Lett.* **2009**, *9*, 2619.
(32) Singh, A. K.; Yakobson, B. I. *Nano Lett.* **2009**, *9*, 1540.
(33) Zhao, P.; Chauhan, J.; Guo, J. *Nano Lett.* **2009**, *9*, 684.
(34) Kresse, G.; Furthmuller, J. *Comput. Mater. Sci.* **1996**, *6*, 15.
(35) Habenicht, B. F.; Kalugin, O. N.; Prezhdo, O. V. *Nano Lett.* **2008**, *8*, 2510.
(36) Perdew, J. P.; Burke, K.; Ernzerhof, M. *Phys. Rev. Lett.* **1996**, *77*, 3865.
(37) Kresse, G.; Joubert, D. *Phys. Rev. B* **1999**, *59*, 1758.
(38) Casiraghi, C.; Hartschuh, A.; Qian, H.; Piscanec, S.; Georgi, C.; Fasoli, A.; Novoselov, K. S.; Basko, D. M.; Ferrari, A. C. *Nano Lett.* **2009**, *9*, 1433.
(39) Nitzan, A. *Annu. Rev. Phys. Chem.* **2001**, *52*, 681.
(40) Galperin, M.; Ratner, M. A.; Nitzan, A.; Troisi, A. *Science* **2008**, *319*, 1056.
(41) Farmer, D. B.; Golizadeh-Mojarad, R.; Perebeinos, V.; Lin, Y.-M.; Tulevski, G. S.; Tsang, J. C.; Avouris, P. *Nano Lett.* **2009**, *9*, 388.
(42) Schaller, R. D.; Pietryga, J. M.; Klimov, V. I. *Nano Lett.* **2007**, *7*, 3469.
(43) Habenicht, B. F.; Craig, C. F.; Prezhdo, O. V. *Phys. Rev. Lett.* **2006**, *96*, 187401.
(44) Freitag, M.; Steiner, M.; Martin, Y.; Perebeinos, V.; Chen, Z.; Tsang, J. C.; Avouris, P. *Nano Lett.* **2009**, *9*, 1883.
(45) Ishii, H.; Roche, S.; Kobayashi, N.; Hirose, K. *Phys. Rev. Lett.* **2010**, *104*, 116801.
(46) Piskunov, S.; Heifets, E.; Eglitis, R. I.; Borstel, G. *Comput. Mater. Sci.* **2004**, *29*, 165.
(47) Williams, G.; Seger, B.; Kamat, P. V. *ACS Nano* **2008**, *2*, 1487.

DOI: 10.1021/nl9035934 | *Nano Lett.* **2010,** *10,* 3237--3242